

CrossMark  
click for updatesCite this: *Chem. Sci.*, 2015, 6, 1879

# A rationally designed small molecule for identifying an *in vivo* link between metal–amyloid- $\beta$ complexes and the pathogenesis of Alzheimer's disease†

Michael W. Beck,<sup>‡ab</sup> Shin Bi Oh,<sup>‡c</sup> Richard A. Kerr,<sup>b</sup> Hyuck Jin Lee,<sup>ab</sup> So Hee Kim,<sup>c</sup> Sujeong Kim,<sup>c</sup> Milim Jang,<sup>a</sup> Brandon T. Ruotolo,<sup>\*b</sup> Joo-Yong Lee<sup>\*cd</sup> and Mi Hee Lim<sup>\*ae</sup>

Multiple factors, including amyloid- $\beta$  (A $\beta$ ), metals, and reactive oxygen species (ROS), are involved in the development of Alzheimer's disease (AD). Metal ions can interact with A $\beta$  species generating toxic oligomers and ROS *in vitro*; however, the involvement of metal–A $\beta$  complexes in AD pathology *in vivo* remains unclear. To solve this uncertainty, we have developed a chemical tool (L2-b) that specifically targets metal–A $\beta$  complexes and modulates their reactivity (*i.e.*, metal–A $\beta$  aggregation, toxic oligomer formation, and ROS production). Through the studies presented herein, we demonstrate that L2-b is able to specifically interact with metal–A $\beta$  complexes over metal-free A $\beta$  analogues, redirect metal–A $\beta$  aggregation into off-pathway, nontoxic less structured A $\beta$  aggregates, and diminish metal–A $\beta$ -induced ROS production, overall mitigating metal–A $\beta$ -triggered toxicity, confirmed by multidisciplinary approaches. L2-b is also verified to enter the brain *in vivo* with relative metabolic stability. Most importantly, upon treatment of 5XFAD AD mice with L2-b, (i) metal–A $\beta$  complexes are targeted and modulated in the brain; (ii) amyloid pathology is reduced; and (iii) cognition deficits are significantly improved. To the best of our knowledge, by employing an *in vivo* chemical tool specifically prepared for investigating metal–A $\beta$  complexes, we report for the first time experimental evidence that metal–A $\beta$  complexes are related directly to AD pathogenesis.

Received 22nd October 2014  
Accepted 3rd December 2014

DOI: 10.1039/c4sc03239j

www.rsc.org/chemicalscience

## Introduction

Alzheimer's disease (AD), a progressive neurodegenerative disease, is the most common form of dementia afflicting 24 million people worldwide.<sup>1</sup> Despite AD being the sixth leading cause of death in the United States, there are currently no disease modifying treatments; approved therapies only offer symptomatic relief without having an effect on the underlying pathogenesis.<sup>1,2</sup> Development of effective therapeutics has been hindered by the fact that AD pathogenesis is still poorly

understood. Pathologically, AD is characterized by the accumulation of aggregated, misfolded proteins, such as amyloid- $\beta$  (A $\beta$ ) peptides (two major forms exist, A $\beta$ <sub>40</sub> and A $\beta$ <sub>42</sub>).<sup>3,4</sup> The amyloid cascade hypothesis suggests that A $\beta$  is the causative agent in AD;<sup>5</sup> however, the etiology of AD can be multifactorial; of particular interest is the role of A $\beta$  with other factors (*i.e.*, metals) toward AD development.<sup>4,6–11</sup>

High concentrations of Fe, Cu, and Zn (*ca.* low mM) are found within A $\beta$  deposits in *ex vivo* tissues from the AD-afflicted brain.<sup>12,13</sup> These metal ions are observed to coordinate to A $\beta$  peptides *in vitro* forming metal–A $\beta$  complexes which could direct toxicity *via* two possible pathways:<sup>4,6–11,14–19</sup> (i) metals could influence the A $\beta$  aggregation pathways leading to the generation and stabilization of toxic A $\beta$  oligomers;<sup>4,7–9,14</sup> (ii) redox active metal ions (*i.e.*, Cu(I/II) and Fe(II/III)) associated with A $\beta$  are shown to produce reactive oxygen species (ROS) under physiological conditions through Fenton-like reactions.<sup>4,6–11,16–19</sup> Overproduction of ROS by metal–A $\beta$  can result in oxidative stress and eventually neuronal death in the AD-affected brain. Although the reactivity of metal–A $\beta$  (*i.e.*, (i) metal–A $\beta$  aggregation (toxic A $\beta$  oligomer formation) and (ii) redox active metal–A $\beta$ -triggered ROS generation, *vide supra*) has been indicated *in*

<sup>a</sup>Department of Chemistry, Ulsan National Institute of Science and Technology (UNIST), Ulsan 689-798, Republic of Korea. E-mail: mhlim@unist.ac.kr

<sup>b</sup>Department of Chemistry, University of Michigan, Ann Arbor, MI 48109-1055, USA. E-mail: bruotolo@umich.edu

<sup>c</sup>Asan Institute for Life Sciences, Asan Medical Center, Seoul 138-736, Republic of Korea. E-mail: jlee@amc.seoul.kr

<sup>d</sup>Department of Neurology, University of Ulsan College of Medicine, Seoul 138-736, Republic of Korea

<sup>e</sup>Life Sciences Institute, University of Michigan, Ann Arbor, Michigan 48109-2216, USA

† Electronic supplementary information (ESI) available: Experimental section, Tables S1–S3, and Fig. S1–S6. See DOI: 10.1039/c4sc03239j

‡ These authors contributed equally.



*vitro*,<sup>4,6–11,14–19</sup> the direct involvement of metal–A $\beta$  complexes in AD pathogenesis *in vivo* is uncertain.

Metal chelating agents have shown that the interference of metal–A $\beta$  interactions as well as the modulation of metal distribution in the brain could lead to an improvement in AD pathology.<sup>4,19–24</sup> 8-Hydroxyquinoline derivatives have been employed to regulate metal-related neurotoxicity in AD; some small molecules, including clioquinol (CQ) and PBT2, have indicated promising results for possible AD treatment in

clinical trials.<sup>4,22,23</sup> The effects of CQ and PBT2 are mainly from their ability to act as an ionophore to redistribute metal ions in the brain instead of directly disrupting metal–A $\beta$  complexes;<sup>4,19,23–25</sup> thus, these compounds would not be able to directly probe the relation between metal–A $\beta$  complexes and AD pathogenesis. Therefore, chemical tools, termed as metamorphosizers, have been recently developed in order to (i) specifically target metal–A $\beta$  complexes and (ii) alter the interaction between the metal and A $\beta$ , consequently (iii) redirecting the toxic aggregation pathway of metal–A $\beta$  into off-pathway, less toxic unstructured A $\beta$  forms and (iv) reducing metal–A $\beta$ -induced ROS production, which eventually alleviates metal–A $\beta$ -linked toxicity.<sup>4,24</sup>

Herein, we demonstrate that a chemical tool (L2-b, Fig. 1a) stands out as being well suited *in vivo* for identifying the association of metal–A $\beta_{40}$ /A $\beta_{42}$  with AD pathogenesis, through *in vitro* biochemical/biophysical/cytotoxicity/metabolism investigations, as well as *in vivo* brain uptake studies. Our *in vitro* tool specifically interacts with metal–A $\beta$  over metal-free A $\beta$  and generates a ternary L2-b–metal–A $\beta$  complex causing structural compaction, as validated by mass spectrometry (MS) and ion mobility-mass spectrometry (IM-MS). Most significantly, we present the first report that the control of metal–A $\beta$  interaction and reactivity by an *in vivo* chemical tool mitigates amyloid pathology and improves cognitive deficits in the 5XFAD AD mouse model. This robust AD mouse model develops severe amyloid pathology and cognitive decline at an early age through high expression of three familial mutant types of human amyloid precursor protein (hAPP; Swedish, Florida, and London) and two mutant forms of presenilin (PSEN1; M146L and L286V).<sup>26</sup> Overall, our studies establish strong experimental evidence for an *in vivo* link between metal–A $\beta$  and AD development, implying that targeting metal–A $\beta$  complexes could be an effective strategy for the future development of new therapeutics.

## Results and discussion

### Design principle and characterization of a chemical tool for investigating metal–A $\beta$ complexes *in vivo*

L2-b (Fig. 1a) was designed to target metal–A $\beta$  complexes and modulate their interaction/reactivity with subsequent reduction of toxicity,<sup>27</sup> in order to determine whether they are connected with AD pathology. For *in vivo* applications, first, chemical tools for this purpose must have specificity toward metal–A $\beta$  complexes in order to limit the disruption of other metalloproteins.<sup>4,24</sup> This property can be imparted into small molecules by using inorganic chemistry concepts to allow specificity for disease-relevant metal ions (Fe(II/III), Cu(I/II), and Zn(II)), along with limiting the metal binding affinity ( $K_d$ ) to  $\geq 10^{-10}$  M, and by including structural components for A $\beta$  interaction.<sup>4,24</sup> To satisfy this aspect, L2-b (a bidentate ligand; Fig. 1a) was constructed upon incorporation of two nitrogen donor atoms (for metal chelation) into the structure of an A $\beta$  aggregate imaging agent (stilbene derivative; for A $\beta$  interaction),<sup>28</sup> which could interact with metal–A $\beta$  complexes (Fig. 1a).<sup>27</sup> L2-b is shown to have apparent  $K_d$  values of *ca.*  $10^{-10}$  and  $10^{-6}$  M for

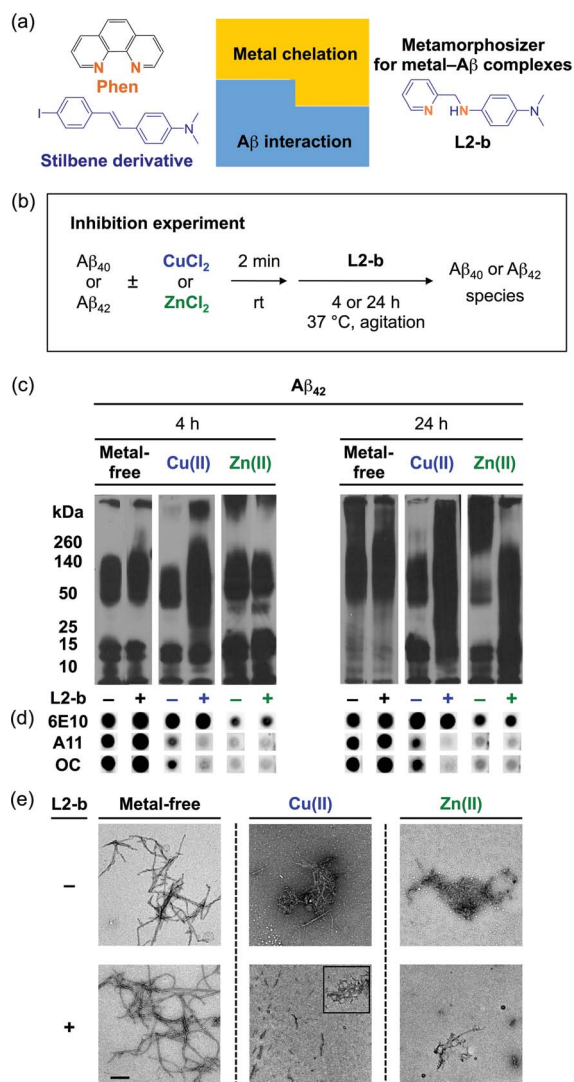


**Fig. 1** Design principle of L2-b and its effect on metal-free and metal-induced A $\beta$  aggregation. (a) Design principle of L2-b, a metamorphosizer for metal–A $\beta$  complexes: a metal binding site (orange) is incorporated into an A $\beta$  interacting framework (blue). (b) Scheme showing the inhibition experiment: metal-free or metal-treated [CuCl<sub>2</sub> (blue) or ZnCl<sub>2</sub> (green)] A $\beta_{40}$ /A $\beta_{42}$  was incubated with (+) or without (–) L2-b for 4 h (left) and 24 h (right). Conditions: [A $\beta$ ] = 25  $\mu$ M; [Cu(II) or Zn(II)] = 25  $\mu$ M; [L2-b] = 50  $\mu$ M; pH 6.6 (for Cu(II) samples) or pH 7.4 (for metal-free and Zn(II) samples); 37 °C; constant agitation. (c) Analysis of the size distribution of the resultant A $\beta_{42}$  species by gel electrophoresis and Western blotting with an anti-A $\beta$  antibody (6E10). (d) Dot blot analysis of the resulting A $\beta_{42}$  species employing 6E10, an anti-A $\beta$  oligomer antibody (A11), and an anti-A $\beta$  fibril antibody (OC). (e) TEM images of the 24 h incubated samples (scale bar = 200 nm).



Cu(II) and Zn(II), respectively, and is relatively selective for Cu(II) over other biologically relevant bivalent ions.<sup>27</sup> Secondly, the blood–brain barrier (BBB) permeability of **L2-b** is critical for applications in the brain, which was first predicted by considering Lipinski's rules of drug-likeness and observing calculated log BB values.<sup>27</sup> Employing CD1 mice, *in vivo* brain uptake studies of **L2-b** newly confirmed its BBB penetration. **L2-b** (ca. 250 ng g<sup>-1</sup>) is observed to be available in the brain when administered by oral gavage (10 mg kg<sup>-1</sup>) to the mice (Table S1†). Thirdly, the metabolic stability of **L2-b** for *in vivo* applications was also verified utilizing human liver microsomes. Susceptibility of **L2-b** to metabolism is between 30 min and 120 min indicating that this compound has moderate metabolic stability, suggesting its suitability for use *in vivo*. Lastly, **L2-b** acts as an antioxidant as well as an inhibitor of Cu(I/II)- or Cu(I/II)-A $\beta$ -induced ROS production as presented in previous studies.<sup>27,29</sup> From our newly performed study using the Trolox equivalent antioxidant capacity in a cellular environment (*i.e.*, murine neuroblastoma Neuro-2a (N2a) cell lysates),<sup>30</sup> **L2-b** exhibits a greater free radical scavenging capacity ( $2.3 \pm 0.2$ ) than Trolox ( $1.0 \pm 0.1$ ), a known antioxidant vitamin E analogue. Therefore, **L2-b** is clearly demonstrated to be viable for *in vivo* use as a chemical tool for exploring the association of metal-A $\beta$  complexes with AD pathogenesis.

### Specific modulation of metal-induced over metal-free A $\beta$ aggregation pathways *in vitro*

To elucidate whether **L2-b** could redirect metal-A $\beta$  aggregation into off-pathway amorphous A $\beta$  aggregates, suggested to be less toxic or nontoxic,<sup>31</sup> while leaving metal-free A $\beta$  cases unaffected, inhibition (Fig. 1b) and disaggregation (Fig. S1a†) experiments<sup>30</sup> were performed employing A $\beta_{40}$  and A $\beta_{42}$ , the two main A $\beta$  forms found in the AD-affected brain. The influence of **L2-b** on both metal-free and metal-mediated A $\beta$  aggregation was monitored at short and long incubation time points.<sup>32</sup> Gel electrophoresis and Western blotting (gel/Western blot, utilizing an anti-A $\beta$  antibody, 6E10)<sup>30</sup> were conducted to determine the molecular weight (MW) distribution of the resulting A $\beta$  aggregates. Dot blot analysis with an anti-A $\beta$  oligomer antibody A11<sup>33</sup> and an anti-A $\beta$  fibril antibody OC,<sup>34</sup> along with 6E10, was carried out to identify the type of A $\beta$  species produced. Moreover, transmission electron microscopy (TEM) images were taken to visualize the morphologies of the resultant A $\beta$  aggregates.<sup>30</sup>

Both the inhibition and disaggregation experiments indicate that **L2-b** does not modulate the aggregation pathways of both A $\beta_{40}$  and A $\beta_{42}$  under metal-free conditions after either short or long incubation periods. Nearly identical MW distributions of the A $\beta$  species in the absence and presence of **L2-b** were observed in the gel/Western blots (Fig. 1c, S1b, and S2a†). The dot blots of the inhibition samples indicated A11 (oligomer)- and OC (fibril)-positive aggregates for metal-free A $\beta_{40}$ /A $\beta_{42}$  even when treated with **L2-b** (Fig. 1d and S2b†). TEM images revealed that A $\beta$  fibrils were mainly present in both the inhibition and disaggregation experiments of metal-free A $\beta_{40}$ /A $\beta_{42}$  with and without **L2-b** after 24 h of incubation (Fig. 1e, S1c, and S2c†).

Thus, metal-free A $\beta$  aggregation is not noticeably influenced upon treatment with **L2-b**.

In contrast to the metal-free conditions, significantly noticeable changes in the metal [Cu(II) or Zn(II)]-induced A $\beta_{40}$  and A $\beta_{42}$  aggregation pathways by **L2-b** were observed compared to **L2-b**-untreated analogues. In both the inhibition and disaggregation experiments, after 24 h of incubation of the Cu(II)-A $\beta$  species with **L2-b**, the resulting peptide species with a wide range of MWs were visualized by gel/Western blot (Fig. 1c, S1b, and S2a†). In the inhibition studies of both A $\beta_{40}$  and A $\beta_{42}$ , as well as in the disaggregation experiment of A $\beta_{42}$ , Cu(II)-A $\beta$  samples treated with **L2-b** even for 4 h also exhibited the distinct MW distribution of A $\beta$  (Fig. 1c, S1b and S2a†). Distinguishably, **L2-b** was capable of limiting the formation of A11- and OC-positive Cu(II)-induced A $\beta_{40}$ /A $\beta_{42}$  aggregates at both short and longer incubation times (Fig. 1d and S2b†). Morphologies of **L2-b**-incubated Cu(II)-A $\beta$ , analyzed by TEM, displayed both narrower and shorter fibrils, as well as unstructured A $\beta$  aggregates in the inhibition experiments (Fig. 1e and S2c†); while less dense, thinner fibrils were mainly observed in the disaggregation experiments (Fig. S1c†). In the case of Zn(II)-A $\beta$ , **L2-b** could also transform the aggregation pathways (Fig. 1c, S1b, and S2a†). The TEM studies revealed **L2-b**-triggered, smaller amorphous Zn(II)-A $\beta$  aggregates in both the inhibition and disaggregation experiments (Fig. 1e, S1c, and S2c†). Overall, **L2-b** is observed to redirect metal-A $\beta$  aggregation mainly into unstructured A $\beta$  aggregates that are generated *via* the off-pathway aggregation and are known to be less toxic or nontoxic.<sup>31</sup> Thus, **L2-b** could be used as a chemical tool specific for such anti-amyloidogenic activity toward metal-A $\beta$  complexes over metal-free A $\beta$  in this manner.

### Formation of structurally-compact complexes with metal-A $\beta$ not metal-free A $\beta$ *in vitro*

In order to explore the specific interaction of **L2-b** with metal-A $\beta$  over metal-free A $\beta$ , nano-electrospray ionization-MS (nESI-MS) studies were employed (Fig. 2a). When metal-free A $\beta_{40}$  was allowed to react with **L2-b**, no binding events were observed, even with a six fold excess of the ligand (Fig. 2a(ii)). In comparison, incubating a comparatively smaller concentration of **L2-b** with A $\beta_{40}$  and Cu(II) promoted readily observed levels of complexes containing A $\beta_{40}$ , Cu(II), and **L2-b** approximately in the ratio 1 : 2 : 1, supporting the metal specific nature of the interaction (Fig. 2a(iv)). The formation of a ternary complex between **L2-b** and Cu(II)-A $\beta_{40}$  is supported by the previously reported NMR studies of **L2-b** with Zn(II)-A $\beta_{40}$  in solution.<sup>27</sup>

Additionally, another MS signal was observed. This signal corresponds to an intact molecular mass of 89.24 Da less than the full-length A $\beta_{40}$  peptide in good agreement with ternary A $\beta_{40}$ -Cu(II)-**L2-b** complex formation (gray, Fig. 2a(iv)). Tandem MS data (Fig. S3†) and subsequent analysis of the fragment ions indicate that this new signal corresponds to a chemical modification within the first five residues of A $\beta_{40}$  (D<sub>1</sub>A<sub>2</sub>E<sub>3</sub>F<sub>4</sub>R<sub>5</sub>). Given a mass measurement error of  $\pm 1$  Da, and supporting **L2-b** binding experiments performed using an A $\beta_{40}$  F4A sequence variant, as well as acetylated analogs (Fig. S4†), we can eliminate





Fig. 2 Mass spectrometric (MS) and ion mobility-mass spectrometric (IM-MS) analyses of A $\beta$  in the presence of L2-b and/or Cu(II). (a) Comparison of incubated A $\beta$  4<sup>+</sup> charge states in the samples containing (i) A $\beta$ <sub>40</sub> (18  $\mu$ M) alone and A $\beta$ <sub>40</sub> co-incubated with (ii) excess L2-b (120  $\mu$ M), (iii) Cu(II) (40  $\mu$ M), and (iv) both L2-b (40  $\mu$ M) and Cu(II) (40  $\mu$ M) [(v) A $\beta$ <sub>42</sub> (pH 9, 18  $\mu$ M) with L2-b (40  $\mu$ M) and Cu(II) (40  $\mu$ M) is also presented]. Consistent with data shown here, the gray signal represents a currently unidentified chemical modification of the N-terminus up to, and including, residue 5 (Fig. S3<sup>†</sup>) but not F4 (Fig. S4<sup>†</sup>). The projected location of the complex consisting of A $\beta$ <sub>42</sub>, Cu(II), and L2-b in a ratio of 1 : 2 : 1 is indicated in pink. (b) IM-MS analysis of A $\beta$ <sub>40</sub> (18  $\mu$ M) incubated in the (i) absence and (ii) presence of L2-b (40  $\mu$ M) and Cu(II) (40  $\mu$ M). Extracted arrival time distributions support the existence of three resolvable structural populations (Collision Cross Section (CCS) data, Table S2<sup>†</sup>).

alterations to F4 as a source of the product observed and show that free primary amines are critical for binding and subsequent A $\beta$  degradation. While no direct observations of the Cu(II)-L2-b-bound A $\beta$ <sub>42</sub> form were indicated by MS, the 89.24 Da

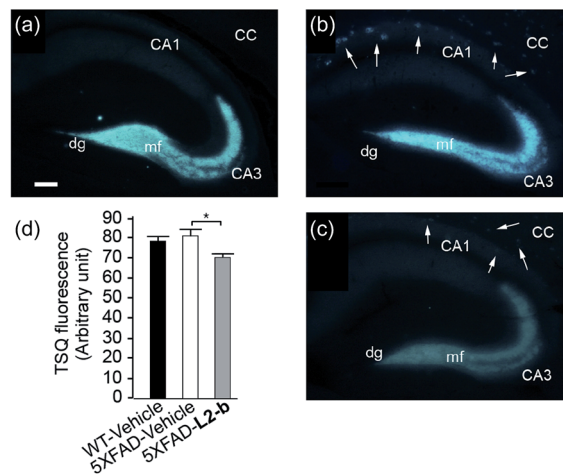


Fig. 3 Levels of Zn(II) in the brain tissues of nontransgenic wild type (WT) and 5XFAD transgenic mice. Amounts of Zn(II) were determined using a fluorescent dye, 6-methoxy-(8-*p*-toluenesulfonamido)quinoline (TSG), in the mossy fiber region (mf) of brains from (a) WT and (b and c) 5XFAD transgenic mice after intraperitoneal administration of (a and b) the vehicle or (c) L2-b (1 mg per kg per day) for three weeks beginning at three months of age (scale bar = 100  $\mu$ m). The fluorescence response of TSG was also shown in the zone of amyloid plaques in 5XFAD mice (shown by arrows; b and c). CC, corpus callosum; CA, cornu amonis; dg, dentate gyrus. (d) The fluorescence intensity of TSG was quantified in the mossy fiber region (mf in a–c) of vehicle-treated WT (black bar;  $n = 6$ ) and 5XFAD male mice (white bar;  $n = 10$ ), or L2-b-treated 5XFAD male mice (gray bar;  $n = 9$ ), where the measurement was performed using five sagittal sections selected randomly from each animal and denoted as an arbitrary unit of the TSG fluorescence [mean  $\pm$  standard error of the mean (S.E.M)]. \* $P < 0.05$  by one-way analysis of variance (ANOVA).

mass loss product was detected (gray, Fig. 2a(v)) upon addition of both L2-b and Cu(II) to the samples, implying the generation of a transient ternary A $\beta$ <sub>42</sub>-Cu(II)-L2-b complex of unknown stoichiometry. These A $\beta$ <sub>40</sub>/A $\beta$ <sub>42</sub> fragmentation results also suggest that, as expected, Cu(II) likely binds to A $\beta$  proximal to the site of L2-b attachment.<sup>4,7</sup> In all cases, neither L2-b nor Cu(II) was detected in complex with the identified A $\beta$  degradation product. Detailed structures of these ternary complexes will be the subject of future studies.

To study the molecular level structural dynamics by which L2-b redirects metal-A $\beta$  aggregation pathways, IM-MS experiments of the complexes produced were performed. A comparison of the arrival time distributions of the metal-free A $\beta$ <sub>40</sub> form with the different ligated states supports an increasing level of structural compaction as additional components (*i.e.*, Cu(II) and L2-b) associate with A $\beta$ <sub>40</sub> (Fig. 2b and Table S2<sup>†</sup>). Analyzing the arrival time distributions for all complex states presented, along with the nESI-MS data, our IM-MS investigations demonstrate that L2-b is capable of specifically interacting with Cu(II)-bound A $\beta$  over metal-free A $\beta$ , subsequently promoting a high level of structural compaction of the complex. This binding of L2-b to metal-A $\beta$  with increased structural compactness could be a key property for the distinguishable reorganization of metal-A $\beta$  aggregation pathways, similar to the previously suggested molecular level mode of action of EGCG toward metal-A $\beta$



complexes which promotes the generation of nontoxic unstructured aggregates *via* off-pathway aggregation.<sup>24,31</sup>

### Targeting and reacting with metal-A $\beta$ complexes in living cells and in the brain of 5XFAD AD mice

The effect of L2-b on metal-A $\beta_{40}$ /A $\beta_{42}$ -induced toxicity was first examined using N2a cells, as an indication of its interaction with metal-A $\beta$  complexes. An increase (*ca.* 10–20%) in cell viability for both A $\beta_{40}$  and A $\beta_{42}$  was displayed upon treatment of cells incubated with Cu(II) or Zn(II), A $\beta$ , and L2-b (10  $\mu$ M each; Fig. S5<sup>†</sup>). Moving forward, the ability of L2-b to penetrate the BBB and interact with metal-A $\beta$  species in the brain was verified in the 5XFAD AD mouse model. Zn(II) found in A $\beta$  plaques was visualized in the brain tissue slices by a fluorophore specific for Zn(II), 6-methoxy-(8-*p*-toluenesulfonamido)quinolone (TSQ; Fig. 3).<sup>35</sup> Administration of L2-b to 5XFAD AD mice intraperitoneally for three weeks on a daily basis starting at the age of three months resulted in drastically diminished fluorescence of TSQ in the plaques (arrows shown in Fig. 3c). Additionally, in

the hippocampal mossy fiber terminals, a Zn(II)-rich region in the brain,<sup>36</sup> there was no difference in the fluorescence of TSQ between wild type and 5XFAD AD mice treated daily with the vehicle, whereas L2-b reduced fluorescence by *ca.* 13% ( $P < 0.05$ ) in 5XFAD AD mice over the same time span (Fig. 3d). Thus, these *in vivo* studies suggest that L2-b is BBB permeable and can enter the brain to interact with intracerebral metals, including those found in A $\beta$  plaques.

### Reduction of amyloid pathology in 5XFAD AD mice

To identify the direct involvement of metal-A $\beta$  complexes in amyloid pathology leading to improved cognition, the 5XFAD mouse model of AD<sup>26</sup> was chosen. L2-b (1 mg kg<sup>-1</sup>) was injected into nontransgenic littermates (wild type) and 5XFAD AD mice *via* the intraperitoneal route for three weeks on a daily basis starting at the age of three months. All mice survived the consecutive treatments, which rarely caused changes in body weight (Table S3<sup>†</sup>). Necropsy of all major organs in L2-b-treated mice revealed no gross changes.

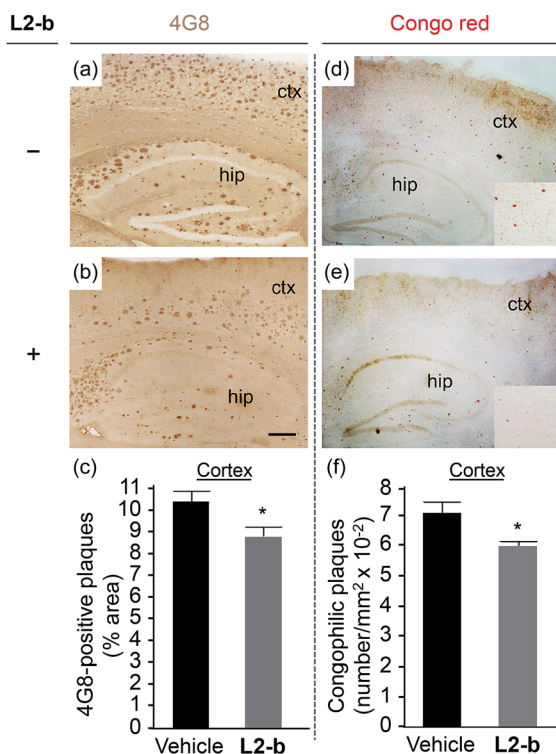


Fig. 4 Effect of daily treatments with L2-b for three weeks on the amyloid deposits in the brains of 5XFAD male mice. Representative microscopic images of (a and b) 4G8-immunostained or (d and e) Congo red stained brain sections of 5XFAD mice, which were given daily (a and d) the vehicle or (b and e) L2-b (1 mg per kg per day) *via* intraperitoneal injection for three weeks starting at three months of age (magnification = 40 $\times$ ; scale bar = 100  $\mu$ m). Inset in (d) and (e): enlarged micrographs of congophilic amyloid plaques in the cortical area (magnification, 400 $\times$ ; hip, hippocampus; ctx, cortex). To evaluate the amyloid pathology of the vehicle (black bars;  $n = 5$ )- or L2-b (gray bars;  $n = 7$ )-treated male 5XFAD mice, (c) the load of 4G8-immunoreactive amyloid deposits and (f) the number of congophilic amyloid plaques in the cortex were measured in five brain sections taken from each animal. \* $P < 0.05$  by one-way ANOVA.

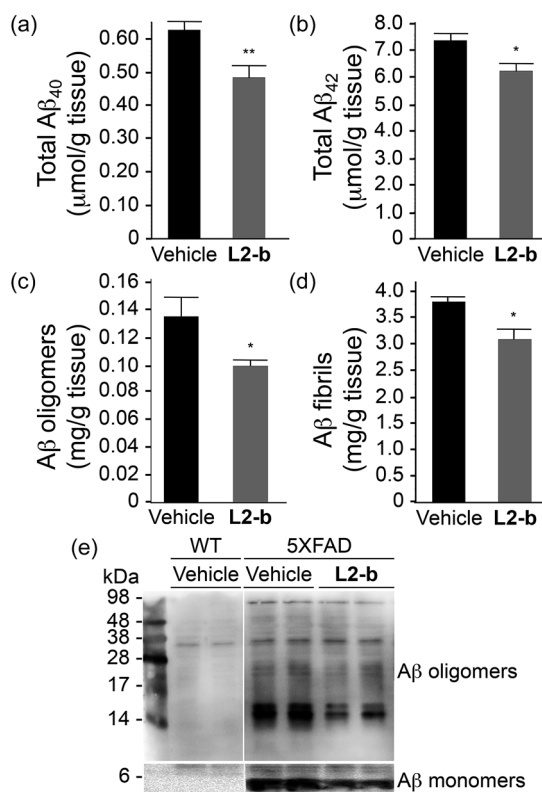


Fig. 5 Levels of A $\beta$  in whole brain tissues of three-month-old male 5XFAD mice. The amounts of (a) total A $\beta_{40}$ , (b) total A $\beta_{42}$ , (c) PBS-soluble A $\beta$  oligomers, and (d) A $\beta$  fibrils were assessed using ELISA after three weeks of treatment with vehicle (black bars;  $n = 5$ ) or L2-b (1 mg per kg per day; gray bars;  $n = 7$ ). Bars denote the levels of A $\beta$ , which were calculated from three independent experiments and expressed as values per gram of tissue. \* $P < 0.05$  or \*\* $P < 0.01$  by one-way ANOVA. (e) 4–20% (lower panels) and 16.5% (upper panels) tris-glycine gel/Western blot analyses were performed to visualize the A $\beta$  monomers and aggregates, respectively, in the brain tissue lysates of wild type (WT; left panels) and 5XFAD male mice (right panels).



The potential association of **L2-b** with amyloid pathology was investigated by first observing the amyloid plaque load in the brain tissue of 5XFAD AD mice. When the brain tissue slices of **L2-b**-administered 5XFAD AD mice were stained with an APP/ $A\beta$ -specific antibody (4G8) or a compact core amyloid plaque indicator (Congo red), it was found that the amyloid plaque burden was ameliorated (Fig. 4). Reduction (*ca.* 15%) of both the area of 4G8-immunoreactive deposits and the number of congophilic amyloid plaques was revealed in the cortex of **L2-b**-treated 5XFAD AD mice when compared to vehicle-treated 5XFAD AD mice (Fig. 4c and f). The changes in the amount of both  $A\beta_{40}$  and  $A\beta_{42}$  in the brain tissues of 5XFAD AD mice following **L2-b** administration were also assessed. Total amounts of  $A\beta$  peptides were analyzed by an enzyme-linked immunosorbent assay (ELISA) in sodium dodecyl sulfate (SDS)- and formic acid (FA)-soluble brain tissue lysates (Fig. 5a and b and S6†), as well as oligomeric and fibrillar  $A\beta$  aggregates in the phosphate buffered saline (PBS)-soluble fraction (Fig. 5c and d).<sup>37</sup> Relative to vehicle-treated 5XFAD mice, the **L2-b**-treated 5XFAD mice showed diminished cerebral levels of both  $A\beta_{40}$  and  $A\beta_{42}$  in all fractions (*ca.* 15–20%,  $P < 0.05$ , Fig. 5a and b). Oligomeric and fibrillar  $A\beta$  species in the PBS fraction were additionally abated by 27% and 15%, respectively ( $P < 0.05$ , Fig. 5c and d). Similarly, the overall reduction of  $A\beta$  species was also indicated by gel/Western blot, where  $A\beta$  monomers and oligomers were noticeably decreased in brain tissue lysates from **L2-b**-treated 5XFAD AD mice (Fig. 5e). Together, these studies demonstrate that daily administration of **L2-b** to the AD

model mitigates amyloid pathology in AD, including the load of amyloid plaque deposits and the levels of a wide range of conformations from monomers to fibrils.

### Cognitive improvement in 5XFAD AD mice

Investigation of behavioral performance was carried out by administering **L2-b** to 5XFAD AD mice which suffer from deficits in learning and memory capabilities as amyloid pathology progresses.<sup>26</sup> The Morris water maze was used to evaluate different aspects of spatial learning and memory in three-month-old 5XFAD AD mice.<sup>26</sup> The wild type mice, which were consecutively injected with vehicle during the experimental period, normally took shorter times upon repetition of the training trial to find the escape platform, located in the north-west (NW) quadrant (Fig. 6a and b). In contrast, vehicle-treated 5XFAD AD mice spent longer times searching for and reaching the platform indicating they had difficulties with learning and memory (Fig. 6). Administration of **L2-b** to 5XFAD AD mice led to a remarkable improvement in the performance of the task. **L2-b**-treated 5XFAD AD mice were capable of finding the target in a comparable time to the wild type mice displaying significantly better memory and learning abilities than their untreated 5XFAD AD littermates ( $P < 0.05$ , Fig. 6a and b). Additionally, **L2-b**-treated 5XFAD AD mice took a more direct and easier path than the vehicle-treated 5XFAD AD mice to search for the platform ( $P < 0.05$ , Fig. 6c). Therefore, **L2-b**, a chemical reagent specific for metal- $A\beta$ , ameliorates cognitive defects in the AD mouse model, along with the attenuation of amyloid pathology.

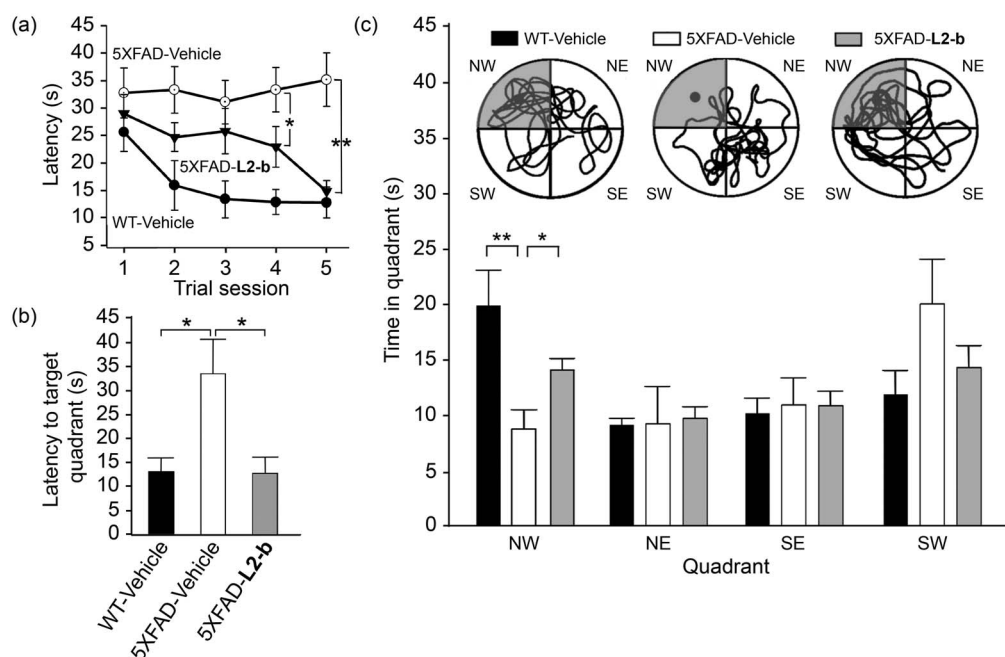


Fig. 6 Learning and memory abilities of three-month-old male wild type (WT) and 5XFAD male mice treated with vehicle (black and white bars) and **L2-b** (gray), measured using the Morris water maze task. (a) The escape latency time was counted every day during the period of the 21<sup>st</sup>–25<sup>th</sup> daily treatments of either vehicle or **L2-b** and the probe trials were performed on the day of the final 25<sup>th</sup> treatment to measure (b) how quickly the mice reach and (c) how long they spend in the target quadrant (NW, highlighted in gray; circles show images of the representative tracks of the mice in the water maze). \* $P < 0.05$  or \*\* $P < 0.01$  by one-way ANOVA ( $n = 6, 13$ , and 14 for vehicle-treated WT and vehicle-/**L2-b**-treated 5XFAD mice, respectively).



These overall *in vivo* observations and results indicate that metal- $\text{A}\beta$  complexes could be directly linked to AD pathogenesis.

## Conclusions

In summary, for the first time, experimental evidence affirms that metal- $\text{A}\beta$  complexes can be directly associated with AD pathogenesis, by applying the first *in vivo* chemical tool which specifically targets metal- $\text{A}\beta$  complexes and ameliorates metal- $\text{A}\beta$  reactivity (*i.e.*, metal- $\text{A}\beta$  aggregation, formation of toxic oligomers, and ROS production) in 5XFAD AD mice. Our findings presented herein demonstrate the feasibility of developing small molecules as *in vivo* chemical tools for studying metal- $\text{A}\beta$ . In addition, our studies indicate that research efforts toward understanding metal- $\text{A}\beta$ -induced pathological pathways and identifying interrelated partners with metal- $\text{A}\beta$  in AD onset and progression at the molecular level should continue to be made. The current and future outcomes, obtained from metal- $\text{A}\beta$ -involved AD research, can open new directions for our long-term goal, the discovery of effective drugs for this fatal neurological disorder.

## Acknowledgements

This work was supported by the Ruth K. Broad Biomedical Foundation, the 2013 Research Fund (Project Number 1.130068.01) of Ulsan National Institute of Science and Technology (UNIST), and the National Research Foundation of Korea (NRF) grant funded by the Korean government (MSIP) (NRF-2014R1A2A2A01004877) (to M.H.L.); the Korea Healthcare Technology R&D Project, Ministry for Health and Welfare, Republic of Korea (A092042) and the Basic Science Research Program, National Research Foundation of Korea, Ministry of Education, Republic of Korea (NRF-2012R1A1A2006801) (to J.-Y.L.); the University of Michigan Protein Folding Disease Initiative (to B.T.R. and M.H.L.).

## Notes and references

- 1 K. Fargo and L. Bleiler, *Alzheimer's Dementia*, 2014, **10**, e47–e92.
- 2 A. Corbett, J. Pickett, A. Burns, J. Corcoran, S. B. Dunnett, P. Edison, J. J. Hagan, C. Holmes, E. Jones, C. Katona, I. Kearns, P. Kehoe, A. Mudher, A. Passmore, N. Shepherd, F. Walsh and C. Ballard, *Nat. Rev. Drug Discovery*, 2012, **11**, 833–846.
- 3 R. Jakob-Roetne and H. Jacobsen, *Angew. Chem., Int. Ed.*, 2009, **48**, 3030–3059.
- 4 M. W. Beck, A. S. Pithadia, A. S. DeToma, K. J. Korshavn and M. H. Lim, in *Ligand Design in Medicinal Inorganic Chemistry*, ed. T. Storr, Wiley, Chichester, 2014, ch. 10, pp. 256–286.
- 5 J. A. Hardy and G. A. Higgins, *Science*, 1992, **256**, 184–185.
- 6 K. J. Barnham, C. L. Masters and A. I. Bush, *Nat. Rev. Drug Discovery*, 2004, **3**, 205–214.
- 7 K. P. Kepp, *Chem. Rev.*, 2012, **112**, 5193–5239.
- 8 M. G. Savelieff, S. Lee, Y. Liu and M. H. Lim, *ACS Chem. Biol.*, 2013, **8**, 856–865.
- 9 H. J. Lee, K. J. Korshavn, A. Kochi, J. S. Derrick and M. H. Lim, *Chem. Soc. Rev.*, 2014, **43**, 6672–6682.
- 10 M. A. Greenough, J. Camakaris and A. I. Bush, *Neurochem. Int.*, 2013, **62**, 540–555.
- 11 A. S. DeToma, S. Salamekh, A. Ramamoorthy and M. H. Lim, *Chem. Soc. Rev.*, 2012, **41**, 608–621.
- 12 M. A. Lovell, J. D. Robertson, W. J. Teesdale, J. L. Campbell and W. R. Markesbery, *J. Neurol. Sci.*, 1998, **158**, 47–52.
- 13 E. L. Que, D. W. Domaille and C. J. Chang, *Chem. Rev.*, 2008, **108**, 1517–1549.
- 14 J. H. Viles, *Coord. Chem. Rev.*, 2012, **256**, 2271–2284.
- 15 T. R. Young, A. Kirchner, A. G. Wedd and Z. Xiao, *Metallomics*, 2014, **6**, 505–517.
- 16 S. Ayton, P. Lei and A. I. Bush, *Free Radical Biol. Med.*, 2013, **62**, 76–89.
- 17 A. S. Pithadia and M. H. Lim, *Curr. Opin. Chem. Biol.*, 2012, **16**, 67–73.
- 18 P. Faller, C. Hureau and G. La Penna, *Acc. Chem. Res.*, 2014, **47**, 2252–2259.
- 19 P. J. Crouch, A. R. White and A. I. Bush, *FEBS J.*, 2007, **274**, 3775–3783.
- 20 C. Rodríguez-Rodríguez, M. Telpoukhovskaia and C. Orvig, *Coord. Chem. Rev.*, 2012, **256**, 2308–2332.
- 21 L. R. Perez and K. J. Franz, *Dalton Trans.*, 2010, **39**, 2177–2187.
- 22 C. W. Ritchie, A. I. Bush, A. Mackinnon, S. Macfarlane, M. Mastwyk, L. MacGregor, L. Kiers, R. Cherny, Q.-X. Li, A. Tammer, D. Carrington, C. Mavros, I. Volitakis, M. Xilinas, D. Ames, S. Davis, K. Beyreuther, R. E. Tanzi and C. L. Masters, *Arch. Neurol.*, 2003, **60**, 1685–1691.
- 23 P. A. Adlard, R. A. Cherny, D. I. Finkelstein, E. Gautier, E. Robb, M. Cortes, I. Volitakis, X. Liu, J. P. Smith, K. Perez, K. Laughton, Q.-X. Li, S. A. Charman, J. A. Nicolazzo, S. Wilkins, K. Deleva, T. Lynch, G. Kok, C. W. Ritchie, R. E. Tanzi, R. Cappai, C. L. Masters, K. J. Barnham and A. I. Bush, *Neuron*, 2008, **59**, 43–55.
- 24 M. G. Savelieff, A. S. DeToma, J. S. Derrick and M. H. Lim, *Acc. Chem. Res.*, 2014, **47**, 2475–2482.
- 25 A. M. Mancino, S. S. Hindo, A. Kochi and M. H. Lim, *Inorg. Chem.*, 2009, **48**, 9596–9598.
- 26 H. Oakley, S. L. Cole, S. Logan, E. Maus, P. Shao, J. Craft, A. Guillozet-Bongaarts, M. Ohno, J. Disterhoft, L. V. Eldik, R. Berry and R. Vassar, *J. Neurosci.*, 2006, **26**, 10129–10140.
- 27 J.-S. Choi, J. J. Braymer, R. P. R. Nanga, A. Ramamoorthy and M. H. Lim, *Proc. Natl. Acad. Sci. USA*, 2010, **107**, 21990–21995.
- 28 H. F. Kung, C.-W. Lee, Z.-P. Zhuang, M.-P. Kung, C. Hou and K. Plössl, *J. Am. Chem. Soc.*, 2001, **123**, 12740–12741.
- 29 M. G. Savelieff, Y. Liu, R. R. P. Senthamarai, K. J. Korshavn, H. J. Lee, A. Ramamoorthy and M. H. Lim, *Chem. Commun.*, 2014, **50**, 5301–5303.
- 30 S. Lee, X. Zheng, J. Krishnamoorthy, M. G. Savelieff, H. M. Park, J. R. Brender, J. H. Kim, J. S. Derrick, A. Kochi, H. J. Lee, C. Kim, A. Ramamoorthy, M. T. Bowers and M. H. Lim, *J. Am. Chem. Soc.*, 2014, **136**, 299–310.



- 31 S.-J. Hyung, A. S. DeToma, J. R. Brender, S. Lee, S. Vivekanandan, A. Kochi, J.-S. Choi, A. Ramamoorthy, B. T. Ruotolo and M. H. Lim, *Proc. Natl. Acad. Sci. USA*, 2013, **110**, 3743–3748.
- 32 As presented in ref. 27, the initial aggregation studies using **L2-b** were conducted only for metal-induced A $\beta_{40}$  aggregation at one incubation time (*i.e.*, 24 h).
- 33 R. Kaye, E. Head, J. L. Thompson, T. M. McIntire, S. C. Milton, C. W. Cotman and C. G. Glabe, *Science*, 2003, **300**, 486–489.
- 34 R. Kaye, E. Head, F. Sarsoza, T. Saing, C. W. Cotman, M. Neula, L. Margol, J. Wu, L. Breydo, J. L. Thompson, S. Rasool, T. Gurlo, P. Butler and C. G. Glabe, *Mol. Neurodegener.*, 2007, **2**, 18–28.
- 35 C. J. Frederickson, E. J. Kasarskis, D. Ringo and R. E. Frederickson, *J. Neurosci. Methods*, 1987, **20**, 91–103.
- 36 J.-Y. Lee, J. S. Kim, H.-R. Byun, R. D. Palmiter and J.-Y. Koh, *Brain Res.*, 2011, **1418**, 12–22.
- 37 S. B. Oh, C. J. Byun, J.-H. Yun, D.-G. Jo, P. Carmeliet, J.-Y. Koh and J.-Y. Lee, *Neurobiol. Aging*, 2014, **35**, 511–519.

